Pergamon

PII: S0301-9322(96)00056-0

Int. J. Multiphase Flow Vol. 23, No. 2, pp. 283–299, 1997

0301-9322/97 $17.00 + 0.00

TWO-PHASE PRESSURE DROP ACROSS SUDDEN CONTRACTIONS IN DUCT AREAS

J. SCHMIDT[1] and L. FRIEDEL[2]

[1]BASF AG, Sicherheitstechnik, 67056 Ludwigshafen, Germany
[2]TU Hamburg-Harburg, Strömungsmechanik, 21079 Hamburg, Germany

(Received 20 August 1993; in revised form 7 February 1996)

Abstract—A new model to calculate the two-phase pressure drop across a sudden contraction in a duct area was developed and checked against data recently obtained with mixtures of air and water, aqueous glycerol, watery calcium nitrate and with the freon 12. In addition, data available from the open literature are considered. In the model all relevant physical parameters are included and, in contrast to correlations published so far, the entrainment of liquid in the gas stream is taken into consideration. The predictions are validated for a wide range of conditions, pipe diameters and physical properties typically encountered in industrial piping systems. Calculations based on the new approach are sufficiently accurate for engineering purposes. © 1997 Elsevier Science Ltd. All rights reserved.

Key Words: pressure drop, contraction, experiments, film–core-model, contraction coefficient

1. INTRODUCTION

Industrial piping systems are often charged with mixtures of gas/vapor and liquid. A considerable effort is then generally needed to calculate the pressure drop along the flow path. This is particularly true for the flow through piping components, e.g. an abrupt contraction in a duct area, since a detailed physical description of the flow mechanism is still not possible. Hence, pressure drops across pipe contractions are most often roughly estimated—a reliable formula is needed in practice.

Most experiments on the two-phase flow pressure drop referred to in the literature have been carried out with steam/water mixtures. Thus, the physical properties of the fluids were not systematically varied and, additionally, flow parameters like mass flow quality and area ratio have been changed only in minor ranges. Moreover, the influence of the gravity force is unknown, since no data are available for both horizontal and vertical flow under comparable conditions. As a consequence, the recalculation of measured pressure drops by using available models will lead to inadequate results. The equations differ mostly in the definition of the mixture density and a reliable submodel for calculating the contraction coefficient in two-phase flow is lacking. In summary, with the available experimental data it does not seem possible to reliably determine the pressure drop as a function of primary parameters. Further, experimental investigations and theoretical analysis are necessary.

2. FLOW PROCESS AND AXIAL PRESSURE PROFILE IN A PIPE CONTRACTION

In the upper part of figure 1 the boundary streamlines for the flow through a sudden contraction of a duct area are shown. The lower part depicts the path of the static pressure along the flow axis for a steady state flow of an incompressible fluid across a contraction. This conception is based on measurements in single-phase water flow. In a distance of about 1.5 times the entrance-pipe diameter in front of the transitional cross section the flow separates from the inner wall and contracts to a jet with a narrowest cross section immediately behind the transition. Hereafter, the jet enlarges and the main flow reattaches to the pipe wall in a distance of less than 14 times the outlet-pipe diameter, depending on the flow condition. In the contracted flow region the static pressure in the inlet line decreases more rapid than in fully developed flow. In the narrowest cross section—the so-called *vena contracta*—it attains the (locally) smallest value. Then, the pressure

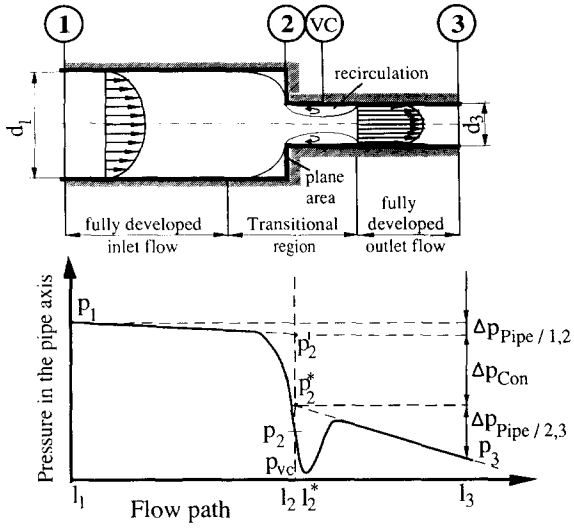

Figure 1. Idealized course of boundary streamlines and pressure in a pipe contraction.

gradually increases and, after reaching its maximum, it merges into the curve of the pipe frictional pressure drop. In the separated flow region eddy zones are developed.

The here considered flow behavior of a nearly incompressible fluid also encompasses gas flow at moderate velocities. At higher gas velocities or in two-phase flow the deviations to the linear pressure course in the region of fully developed flow may be very large; this is especially true for critical, vaporizing flow as shown by the measurements of Rousseau (1987). Whereas at velocities usually encountered in real piping systems the difference is negligible and can be ignored.

In contrast to the well-known axial pressure profile in the transitional region between the flow separation and reattachment for single-phase liquid flow, the pressure profile and the shape of streamlines in two-flow are still unknown; there is not evidence whether or not the profile is similar to the one in gas respectively liquid flow, i.e. it is not known if a flow contraction occurs at all.

The axial pressure profile leads to the pressure drop across a pipe contraction Δp_{con}. It is generally defined as a local change of pressure in the transitional cross section for an assumed fully developed flow for both the inlet and the outlet pipe irrespective of the flow separation. In practice, it can be determined from measured axial pressure profiles in the regions of fully developed pipe flow upstream and downstream of the pipe contraction by extrapolating these (linear) pressure courses to the transitional cross section (Kays 1950).

3. EXPERIMENTAL FACILITY AND TEST PROGRAM

Most of the pressure drop data used in this analysis have been measured by using the test facility shown in figure 2. Liquid is supplied by a centrifugal pump from a storage tank through a pressure compensation vessel and a heat exchanger to a mixer, where the liquid is mixed with air taken from a receiver vessel. This two-phase mixture flows through a horizontal test section of 9 m in length or a vertical test section with a length of 5 m and then back to the storage tank, which simultaneously acts as liquid separator. The separated liquid is recirculated and the air is released.

Each test section used for the experiments was made up by connecting two straight stainless steel pipes, table 1. The tolerance of the inner diameter for the seamless precision pipes was only ± 0.2 mm along the whole pipe length. Ring chambers for the pressure measurements were pasted on the outer wall of each pipe line in distances of 2, 5, 10, 20, 30, 40, 50 and 60 inner diameters from the first flange. The sharpness of the entrance flanges were less then 0.1%, whereby the sharpness is defined as the corner radius of the flange related to the inner pipe diameter. In total, measurements have been taken with eight test sections.

The pressure drop across the pipe contraction has been determined by extrapolating the axial pressure profiles measured along the inlet and outlet pipes. For that, the differential pressure

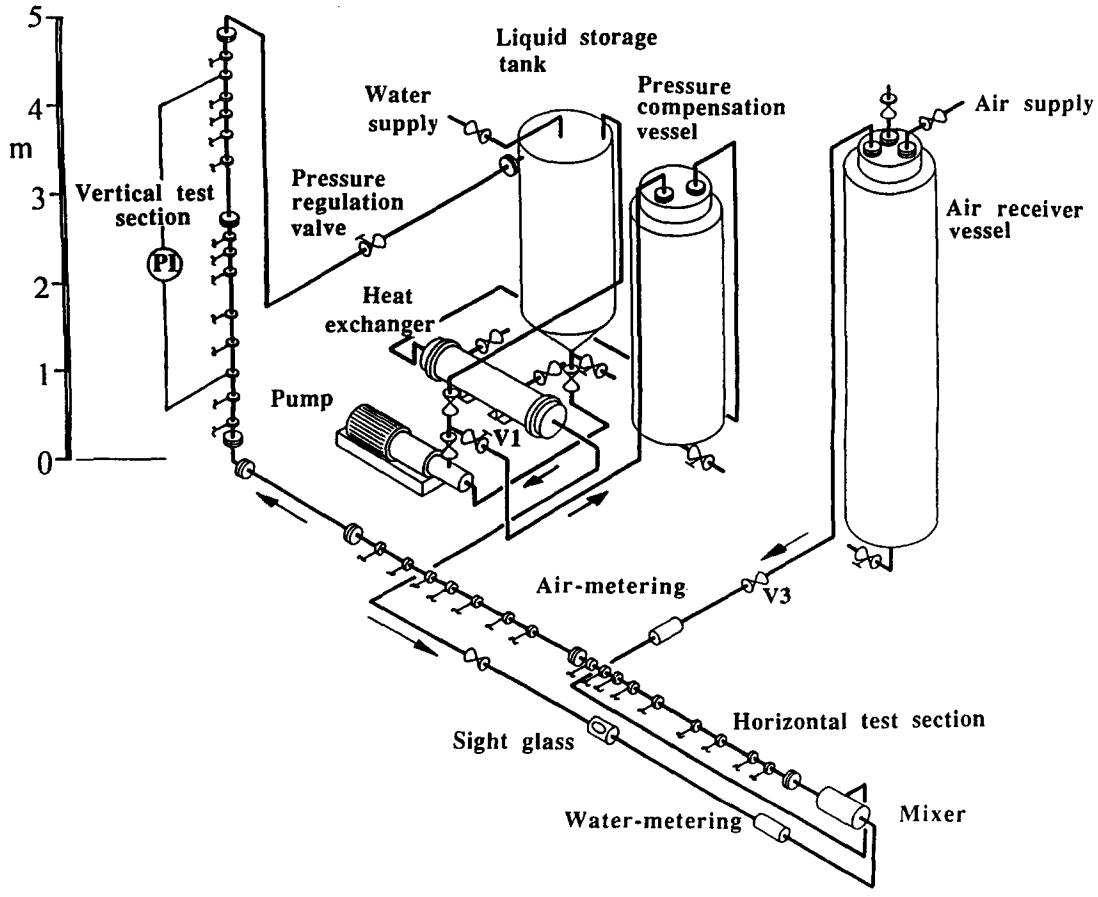

Figure 2. Test facility.

between a reference tap—a certain ring chamber in the inlet pipe—and each ring chamber in the outlet pipe was measured one after the other as a first pressure sequence. Then, a second sequence has been carried the other way round with respect to a reference tap in the outlet pipe. Additionally to these so obtained pressure differences, the static pressure at the reference tap in the inlet pipe was measured. While very precise pressure transducers have been used with uncertainties of less than 0.2, respectively, 3 mbar depending on the measuring range of the transducer, the overall uncertainties of the pressure drop data are higher due to pressure fluctuations typically encountered in two-phase flow. Nevertheless, for most of the results the uncertainty is less than $\pm 5\%$ of the experimentally determined pressure drop.

In the test facility measurements were taken with mixtures of air and water, aqueous glycerol and watery calcium nitrate; liquid phase densities and dynamic viscosities are given in table 2. At a temperature of 25°C—where most of the experiments were performed—the density of the 51 wt%

Table 1. Area ratios of the test sections and inner diameters of inlet and outlet piping

Area ratio A_3/A_1	Inner pipe diameter inlet [mm]	outlet [mm]	
0.057	17.2	72.2	
0.115	19.0	56.0	
0.167	29.5	72.2	
0.180	24.0	56.5	Transparent acrylic
0.276	29.5	56.2	
0.375	44.2	72.2	
0.445	29.5	44.2	
0.619	44.2	56.2	

Table 2. Densities and dynamic viscosities of the test-liquids at a temperature of 25°C

	Water	Aqueous $Ca(NO_3)_2$ 51 wt%	Aqueous Glycerin 79 wt%
Dynamic viscosity [Pas 10^{-3}]	0.890	7.70	43.4
Density [kg/m^3]	997.2	1482	1207

solution of aqueous calcium nitrate is about 50% larger than the density of water, and the viscosity of the 79 wt% glycerol solution is approximately 50 times higher compared to that of water. In conjunction with air, the mass flow quality of these two-component two-phase mixtures remained constant along the test section. For the sake of completeness, the influence of a drop in mass flow quality due to vaporization was studied by additional measurements on another loop with the freon 12 (difluor–dichlor–methane) as a one-component two-phase mixture. With these two-phase mixtures and test sections it was possible to systematically investigate the dependence of the pressure drop on all relevant flow parameters and physical properties in wide ranges. The minimum and maximum boundaries and the mean values of the parameters adjusted in the experiments are given in table 3. Most of the pressure drop data are published by Schmidt (1993). Additionally, there is a more detailed description given of the test facilities and test sections, the procedure of pressure drop measurement and a discussion of the uncertainties.

Beside the measurements on pressure drop further experiments were devoted to identify the location and the size of the vena contracta downstream of a pipe contraction and, subsequently, to estimate the contraction coefficient for two-phase flow. For this, the course of the static pressure along the flow axis has been measured with a piezo-probe in a pipe contraction made from transparent acrylic with an area ratio of 0.1804, i.e. 56.5 mm inner diameter of the inlet pipe and 24 mm inner diameter of the outlet pipe. The piezo-probe with an outer diameter of 1 mm was fixed to a wire with 0.3 mm in diameter, which was moveable installed over a length of about 7000 mm in the center of the vertically directed test section. For the reason of accuracy, with this probe the static pressure was measured as the difference to the pressure at a certain reference tap at the pipe wall. Additionally, a pilot-tube has been used in a radial direction to measure the dynamic pressure in the cross section with the lowest static pressure in the pipe center—here defined as the vena contracta. The photograph in figure 3 depicts the pitot-probe and the assembly to adjust a certain horizontal and vertical position in the outlet pipe of the contraction. Three bores to measure the static pressure along the annular plane are also shown.

4. EXPERIMENTAL RESULTS

As an example, in figure 4 the measured pressure drops in a horizontal air/water flow through a pipe contraction with an area ratio ($\sigma_{3,1} = A_3/A_1$) of 0.0568 are shown as a function of the mass flow quality at mass fluxes of 500 up to 4000 kg/m^2/s. The static pressure immediately upstream of the transitional cross section was 5 bar for all measurements. As expected, the pressure drop steeply increases with higher mass flow quality and mass flux. With an inlet mass flux of 1000 kg/m^2/s the quality could not be increased beyond about 40%, since critical flow condition has been established in the contraction, i.e. the system pressure no longer remained constant but raised with increasing mass flow quality. Distinctly at low mass flow qualities the curves exhibit

Table 3. Parameter ranges of the experiments on pressure drop across sudden contractions

		Minimum	Average	Maximum
Mass flow quality	[%]	0	12	100
Mass flux $\dot{m}_3$	[kg/m^2/s]	50	1825	16000
Area ratio $\sigma_{3,1}$	[-]	0.057	0.1914	0.619
System pressure p_2	[bar]	2	5.7	25
Density of liquid	[kg/m^3]	994	1058	1480
gas/vapor	[kg/m^3]	2.3	6.3	162
Viscosity of liquid	[Pas 10^{-3}]	0.45	3.39	35.45
gas/vapor	[Pas 10^{-3}]	0.007	0.017	0.019
Surface tension	[N/m]	0.064	0.073	0.101

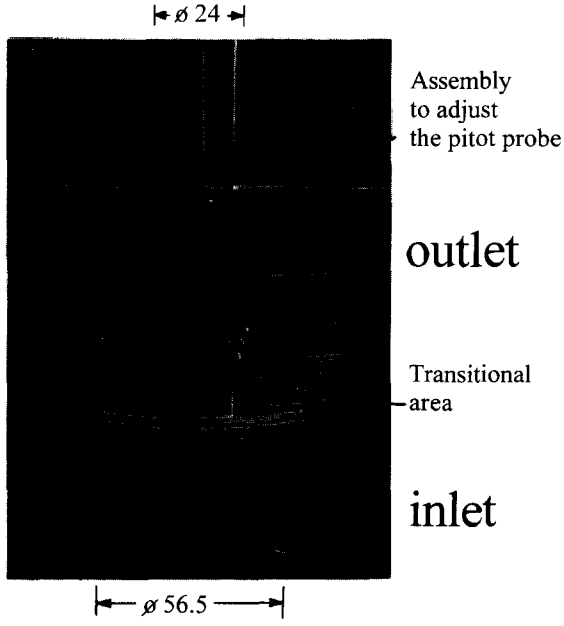

Figure 3. Acrylic pipe contraction with the pitot probe and the bores for measuring the base pressure distribution on the annular plane.

a wavy course. This is not due to measurement errors, but it characterizes a change of flow pattern in the inlet or outlet pipe.

At mass flow qualities below 1% and, therefore, at low up to moderate void fractions the pressure drop strongly depends on the liquid phase density and viscosity; this was shown with measurements of air and aqueous glycerol respectively watery calcium nitrate (Schmidt 1993). Regarding the variation in liquid properties, the largest (relative) differences in pressure drop have been obtained in single-phase liquid flow. In detail, the pressure drop measured with an aqueous glycerin solution is larger than that in pure water flow due to the higher viscosity and, subsequently, the larger frictional pressure loss. The lowest pressure drop was achieved with the flow of an aqueous calcium

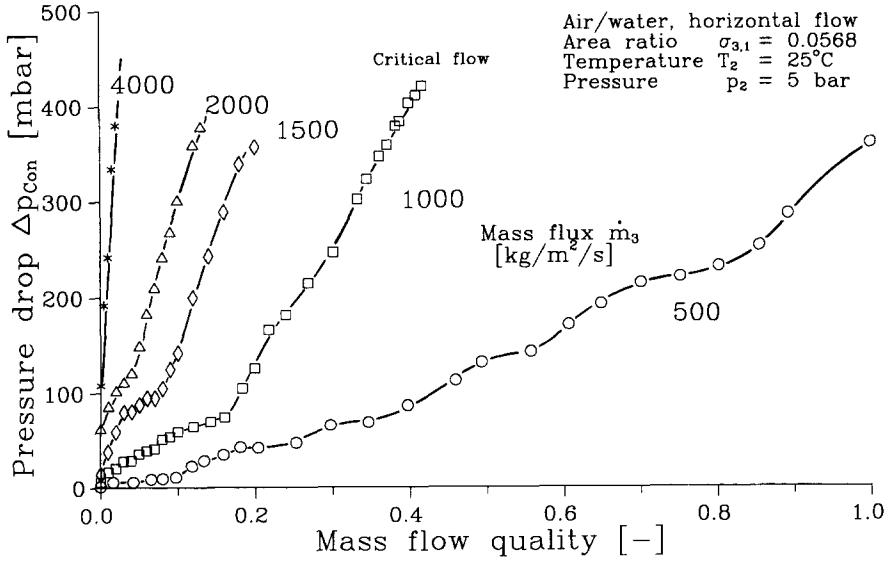

Figure 4. Experimental pressure drop in horizontal air/water flow as a function of mass flow quality and mass flux.

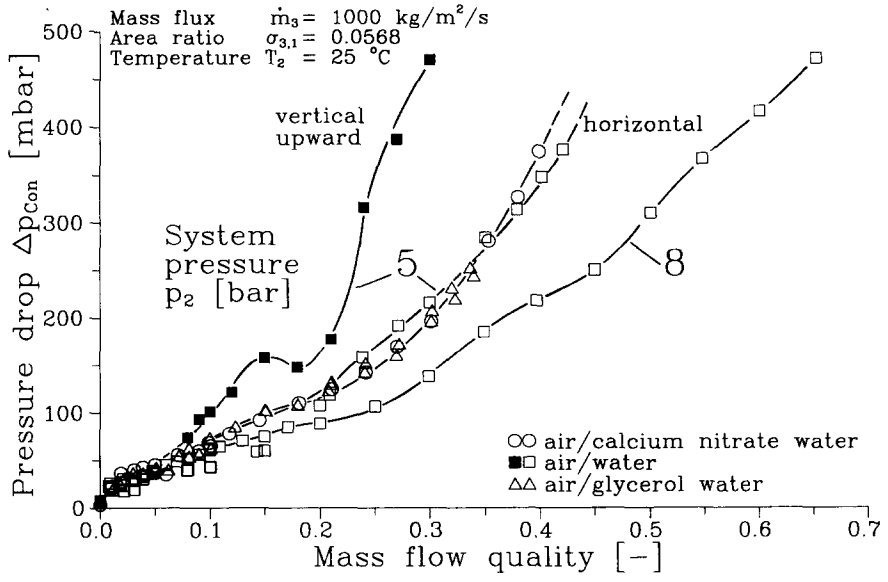

Figure 5. Measured pressure drop as a function of mass flow quality, system pressure and flow direction.

nitrate solution. In comparison to the data obtained in water flow the pressure drop is further decreased as a result of the larger density, although a viscosity is slightly increased,† see table 2.

At mass flow qualities above 1% the void fraction generally exceeds 90% for pressures below 10 bar considered here and, hence, the influence of the liquid phase properties on the pressure drop is lesser. Figure 5 shows, however, that there can be a significant effect of viscosity at low mass flow qualities when it is varied over a wide range. The flow direction—horizontal flow compared to vertically upward flow—generally had only a minor influence (Schmidt 1993). In spite of different flow patterns in horizontal and in vertical upward flow there is no obvious tendency for the influence of flow direction on the pressure drop, i.e. the pressure drop in vertical upward flow may partially be larger or lower than in horizontal flow. Differences of up to 50% between both flow directions have, however, been measured at certain mass flow qualities as shown in figure 5, but in most cases the effect of orientation was lesser (Schmidt 1993).

The location of the vena contracta, defined as the distance to the transitional cross section, and the size of the narrowest flow cross section identified from the course of the static pressure along the flow axis are shown in figures 6 and 7: in single-phase flow of water and of air the pressure curves show an expected minimum in the narrowest flow cross section. The vena contracta is always established at a distance of about 10 mm behind the transitional cross section and depends only slightly on the mass flux; the distance relates to about 0.4 times the upstream-pipe diameter. In two-phase flow at mass flow qualities between approximately 1 and 97% a local pressure minimum was not detectable, figure 8. Comparable results have been obtained with further measurements and mass fluxes up to 4500 kg/m²/s. A (physical) explanation of this phenomenon was delineated from analyzing single pictures of a film taken in a separate transparent glass test section with vertical upward air/water flow: e.g. in annular two-phase flow the liquid wall film flows up the inlet pipe until it reaches the annular plane of the contraction. There, it is dammed up and then radially pushed towards the edge of the outlet pipe, where a thin film is formed, which permanently bursts into fine droplets. These droplets are carried through the near-wall region just behind the pipe

†In single-phase flow the pressure drop across a sudden contraction is often defined as the sum of the accelerational pressure drop in a fictitious frictionless flow and the pressure loss due to friction. While the accelerational pressure drop depends only on the fluid density and geometrical parameters, the frictional pressure loss is, additionally, affected by the viscosity. Regarding the own pressure drop measurements a higher liquid density e.g. of the calcium nitrate solution compared to that of water leads generally to a lower accelerational pressure drop. This is partially compensated by an increased pressure loss due to the larger liquid viscosity. Overall, the total pressure drop is decreased.

In two-phase flow a pressure loss can not be defined as general as in single-phase flow, because it depends on a void fraction model as a closure condition, which has to be empirically determined. Subsequently, it is not recommended to use those ambiguous definitions in two-phase flow.

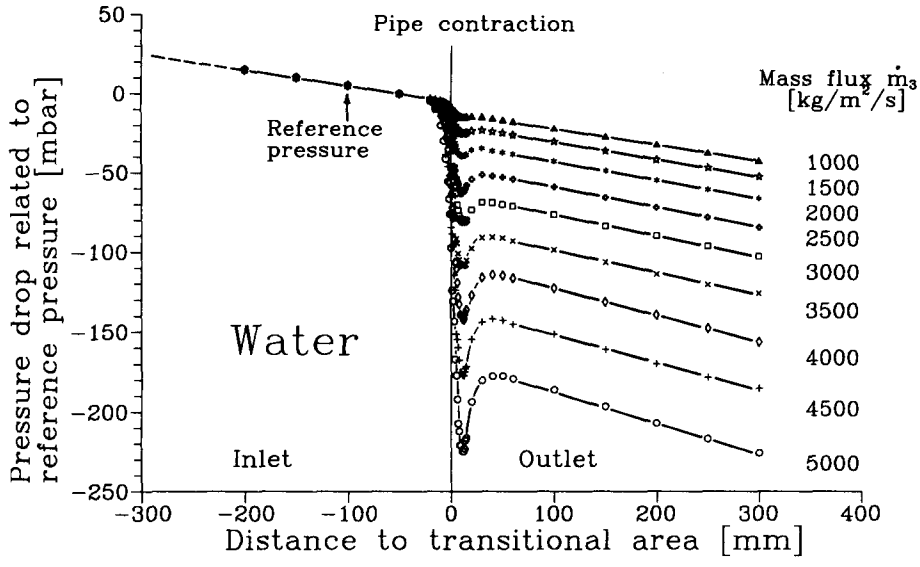

Figure 6. Measured courses of static pressure within the pipe axis in water flow through a contraction with an area ratio of 0.18.

contraction and, as a consequence, recirculation of the fluid further downstream is suppressed. Overall, the measurements of the axial pressure profile indicate that in most gas/liquid flows a (measurable) narrowest cross section is generally not established—the contraction analogy between single-phase and two-phase flow assumed so far for simplicity seems, thus, physically not reasonable in this range of mass flow quality.

The depicted experimental results are validated with extra pressure measurements crosswise to the flow direction at a location, where the vena contracta in single-phase flow was established: In figure 9 the course of the dynamic pressure across the (expected) vena contracta is presented in dependence of the distance from the inner wall of the outlet pipe for an air/water flow through a pipe contraction. A mass flux of 1000 kg/m²/s, mass flow qualities of 2, 5, 7.5% and a system pressure of 2 bar have been adjusted. Mass flow qualities noticeable above these values led to critical flow in the pipe contraction. Starting with the maximum value in the center of the flow cross section the dynamic pressure slowly decreases in the direction to the inner wall without

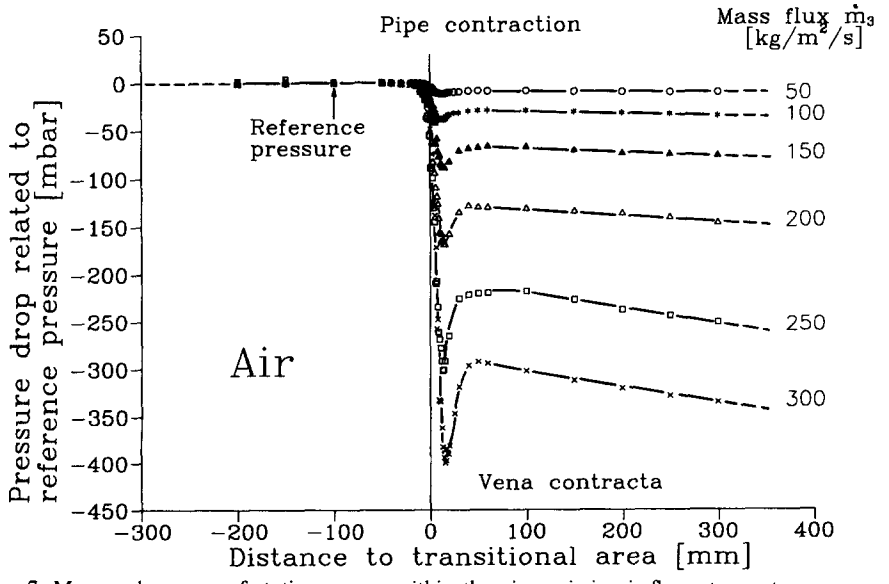

Figure 7. Measured courses of static pressure within the pipe axis in air flow at a system pressure of 2 bar through a contraction with an area ratio of 0.18.

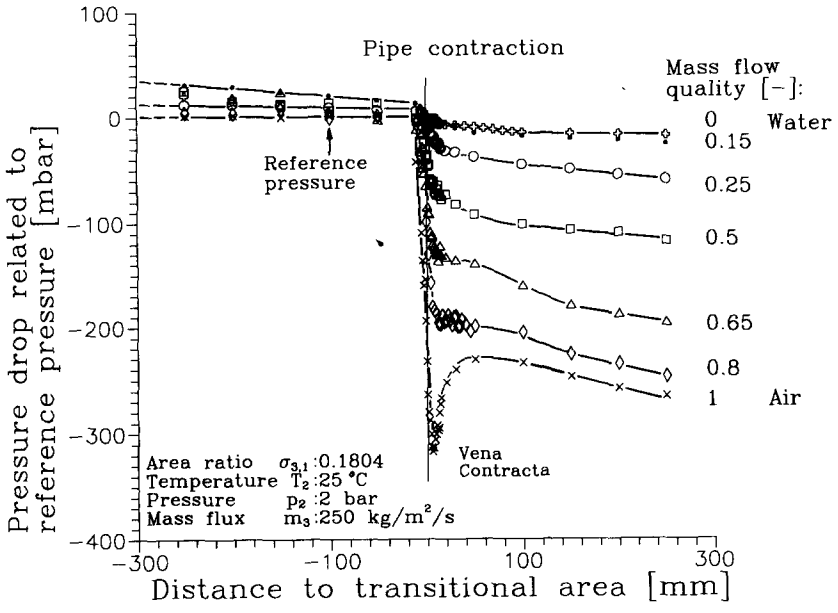

Figure 8. Measured courses of static pressure within the pipe axis in two-phase air/water flow through a pipe contraction.

adopting negative values, which are typically established in single-phase water and air flow. Subsequently, there is no change in flow direction and a zone of recirculation could also not be detected. Unlike single-phase flow, there is no vena contracta measurable in two-phase flow. Herewith, similar presumptions made by Morris (1990) for orifice two-phase flow were now experimentally validated for the flow through a pipe contraction.

5. NEW PRESSURE DROP MODEL

The new approach to predict the two-phase flow pressure drop across a pipe contraction is based on a two-fluid film/core flow model, figure 10. In the inlet pipe a part of the liquid is flowing as a film along the inner wall and surrounds the gas flow in the core; the gas carries the rest of the

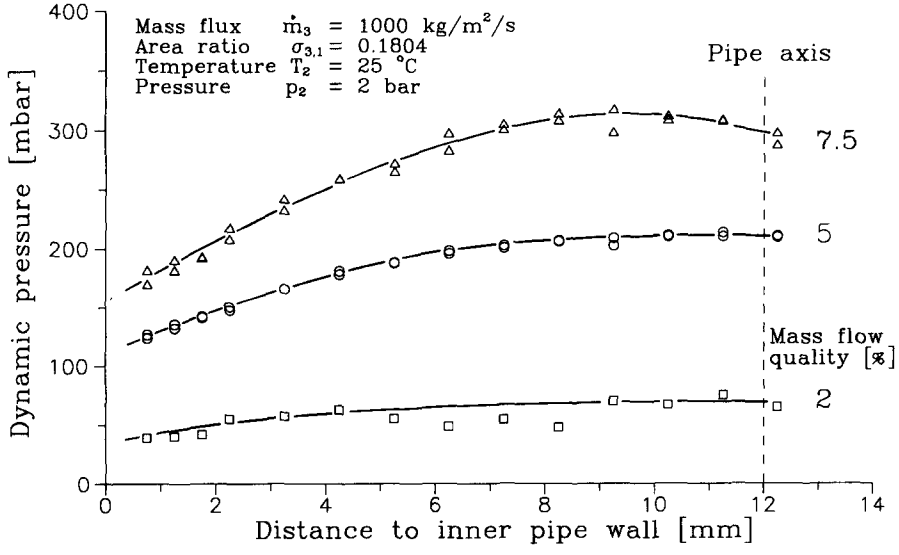

Figure 9. Measured dynamic pressure about 10 mm downstream of the transition area in a pipe contraction for a vertical upward air/water flow.

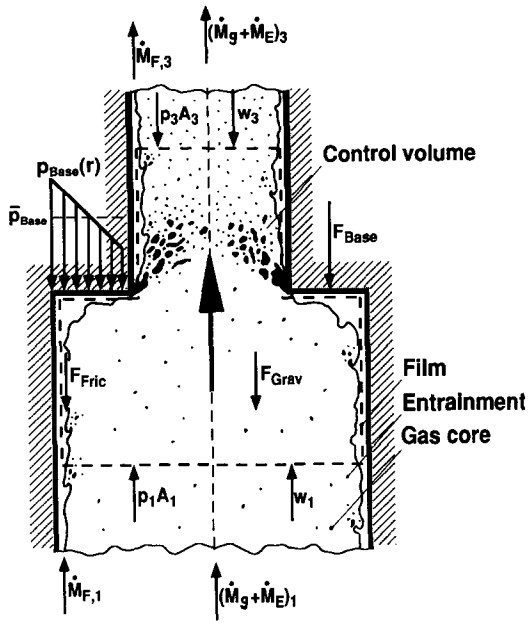

Figure 10. Forces and mass flow rates in a control volume during annular-mist flow.

liquid. When the film has reached the annular plane of the contraction, it is pushed towards the outlet pipe—as observed by analyzing photographs. At the transitional edge the liquid film is splitted into liquid fragments (e.g. rod-shaped or droplets) and is carried away with the gas. Downstream of the contraction some part of the liquid is again deposited to the wall and, subsequently, a film flow is induced in the outlet pipe. For simplicity it is assumed, that the mean velocities of the gas and the herein carried liquid are the same.

Although a film/core model is assumed to evaluate the pressure drop, the model is not restricted to annular flow. Indeed, the whole range of mass flow quality, respectively, flow pattern is covered. Nevertheless, a significant part of the experiments were performed in annular flow—at least in the outlet pipe. At low mass flow qualities, i.e. when other flow pattern will typically be established, the liquid entrainment is supposed to be negligibly small.

The relation to calculate of the pressure drop across the sudden contraction is based on an (integral) momentum balance between pipe cross sections far upstream (subscript 1) respectively far downstream (subscript 3) of the transitional cross section (subscript 2) for a two-phase flow assumed to be in a quasi-steady state:

$$p_1 A_1 - \int_{A_3 - A_1} p_{base}(r)\,\mathrm{d}A - p_3 A_3 - (F_{fric} + F_{grav})_{1,3} = \frac{\dot{m}_3^2}{\rho_{eff,3}} K_{M,3} A_3 - \frac{\dot{m}_1^2}{\rho_{eff,1}} K_{M,1} A_1 \qquad [1]$$

where p_{base} denotes the base pressure (pressure acting on the annular plane of the contraction), $\dot{m}$ the mass flux, ρ_{eff} the mean effective density of the gas/liquid mixture, and K_M denotes the momentum enhancement factor. Accounting for the pressure drop due to friction and gravity in fully developed flow in the inlet $[\Delta p]_{pipe;1,2}$ and outlet pipe section $[\Delta p]_{pipe;3,4}$ (see figure 1)

$$\Delta p_{con} = p_2' - p_2^* = (p_1 - [\Delta p_{fric} + \Delta p_{grav}]_{pipe;1,2}) - (p_3 + [\Delta p_{fric} + \Delta p_{grav}]_{pipe;2,3}) \qquad [2]$$

the basic equation for the pressure drop across the sudden contraction reads as follows:

$$\Delta p_{con} = \dot{m}_3^2 \left(\frac{K_{M,3}}{\rho_{eff,3}} - \frac{K_{M,1}\sigma_{3,1}}{\rho_{eff,1}} \right) + \frac{1}{A_3} (\Delta F_{base} + \Delta F_{fric} + \Delta F_{grav}). \qquad [3]$$

The first term characterizes the drop of momentum flux and the following are the plane reaction forces F_{base} acting on the annular plane of the contraction as well as the friction forces F_{fric} and

the gravity forces F_{grav} for both the flow through the contraction and a (fictitious) fully developed pipe flow. The force terms are defined as

$$\Delta F_{base} = -\int_{A_3 - A_1} (p_1 - p_{base}(r))\mathrm{d}A \quad [4]$$

where $p_{base}(r)$ is the local base pressure, depending on the pipe radius r, and

$$\Delta F_{fric} = F_{fric,1\cdot3} - A_3([\Delta p_{fric}]_{pipe/1,2} + [\Delta p_{fric}]_{pipe/2,3}) \quad [5]$$

$$\Delta F_{grav} = \boldsymbol{g} \sin \Psi(\bar{\rho}_{eff,1/2}A_3(z_3 - z_1) - \{A_1[\rho_{eff}]_{pipe/1,2}(z_2 - z_1) + A_3[\rho_{eff}]_{pipe/2,3}(z_3 - z_2)\}) \quad [6]$$

where $\boldsymbol{g}$ is the gravity constant, and Ψ denotes the inclination of the flow compared to the horizontal, z is the axial flow coordinate.

In turbulent (single-phase) flow the momentum enhancement factor generally approximates a value of unity. Hence, it is no longer taken into consideration. Additionally, the pressure drop due to gravity is neglected, because it was identified to be of minor influence.

5.1. *Effective density of the two-phase mixture*

The mean effective density of the gas/liquid mixture is defined by the total momentum flux $\dot{I}$ within a certain flow cross section

$$\dot{I} = \dot{I}_G + \dot{I}_E + \dot{I}_F = \rho_{eff} w^2 A = \frac{\dot{m}^2}{\rho_{eff}} A. \quad [7]$$

This equals the sum of those of the gas (subscript G) and the herein carried entrained liquid (subscript E) as well as that of the liquid film on the inner pipe wall (subscript F); w is a characteristic mean velocity of the two-phase flow. The momentum flux of gas bubbles eventually

Table 4. New approach for calculating the pressure drop across sudden contractions in duct areas (a calculational example is given by Schmidt 1993)

$$\Delta p_{con} = \frac{\dot{m}_3^2\left[\frac{1}{\rho_{eff,3}} - \frac{\sigma_{3,1}}{\rho_{eff,1}} + f_{con}\rho_{eff,3}\left(\frac{\dot{x}}{\rho_{G,3}\epsilon_3} - \frac{1-\dot{x}}{\rho_L(1-\epsilon_3)}\right)^2(1-\sqrt{\sigma_{3,1}})^2\right]}{1 + \Gamma_{con}\left(\frac{1}{\sigma_{3,1}} - 1\right)} \quad [16]$$

$$\epsilon = 1 - \frac{2(1-\dot{x})^2}{1 - 2\dot{x} + \sqrt{1 + 4\dot{x}(1-\dot{x})\left(\frac{\rho_L}{\rho_G} - 1\right)}} \quad [17]$$

$$\epsilon_E = \frac{1}{S}\left[1 - \frac{(1-\dot{x})}{1 - \dot{x}(1 - 0.18 \cdot We^{0.12} \cdot Re^{0.50})}\right]; \quad S = \frac{\dot{x}}{1-\dot{x}}\frac{1-\epsilon}{\epsilon}\frac{\rho_L}{\rho_G} \quad [18]$$

$$We = \dot{m}^2\dot{x}^2\frac{d}{\rho_G\sigma^*}\frac{(\rho_L - \rho_G)}{\rho_G}; \quad Re = \frac{\dot{m}(1-\dot{x})d}{\eta_L} \quad [19]$$

$$\Gamma_{con} = 0.77\sigma_{3,1}(1 - \sigma_{3,1}^{0.306}) \quad [20]$$

$$f_{con} = 5.2 \cdot 10^{-3}\dot{x}^{0.1}(1-\dot{x})\left(\sigma_{3,1}\frac{\eta_L}{\eta_{G,3}}\right)^{0.8} \quad [21]$$

carried in the film is negligibly small. Rearranging the momentum equation leads to a relationship for the mean effective density (Morris 1984), table 4, [17]. This equation includes among the densities of both phases ρ_G and ρ_L, the mass flow quality $\dot{x}$ and the mean void fraction ϵ a further parameter, the mean volumetric entrainment ϵ_E, in order to take the liquid entrainment into consideration. It is defined as the area occupied only by the entrained liquid related to that one occupied by the whole liquid. For example, an annular flow without entrained droplets is characterized by a volumetric entrainment of zero, whereas a mist flow, with no liquid film on the wall leads to a value of unity. Characteristic boundary limits of the two-phase density are also well described with this equation, e.g. in gas or liquid flow the effective density equals to the respective single-phase density.

The calculation of the effective density requires a model for the mean void fraction in the fully developed flow region of the inlet and outlet pipe. Here, the model of Huq (1990) was chosen†, table 4, [18]. In comparison to other models cited in the literature the reproductive accuracy based on more than 10,000 available experimental data is better (Schmidt 1993). Precautionary, it is recommended not to apply this model for high viscosity fluid flow or mass fluxes less than 50 kg/m^2/s; within this parameter range the equations of HTFS (see Walley and Ward 1981; Rouhani 1974) are significantly more accurate. For more or less aqueous liquids and larger mass fluxes—the typical conditions chosen for the experiments—the calculational results do not differ much from each other.

Models available in the literature for calculating the mean volumetric fraction of the liquid entrained in the gas core ϵ_E are generally valid only for fairly developed two-phase flow in a constant area duct. Indeed, with these models a reliable prediction in a wide parameter range is not attainable. Therefore, a new equation for the mean volumetric liquid entrainment is developed as a function of all primary parameters. Other authors have already shown that the amount of liquid entrained in the gas core may be described as a function of characteristic Reynolds and Weber numbers, whereby the entrainment increases with larger values of both numbers. Following Ishii and Kataoka (1982), the Reynolds number is specified by the superficial velocity and the viscosity of the liquid phase, whereas the Weber number should be defined with the gas core superficial velocity and a density correction term‡, table 4, [20]. Both dimensionless numbers will be fitted into an equation, which *a priori* accounts for the theoretical boundary values of the volumetric liquid entrainment ϵ_E, respectively, the entrainment based on liquid mass flow rates E as following ($E = \dot{M}_E/\dot{M}_L$, where $\dot{M}$ denotes the mass flow rate): in single-phase liquid flow the entrainment should vanish and in gas flow it is supposed to be unity. This follows firstly from the assumption that the last (tiny) bubble remaining at mass flow qualities of nearly zero is enclosed by the liquid as a film and does not contain any droplets. On the other hand, the last (tiny) droplet in a mist flow is carried along the pipe axis and not along the wall as experience shows. In two-phase flow with equal densities of both phases, e.g. in a vapor/liquid mixture at the thermodynamic critical pressure, the entrainment is supposed to approach a boundary value of zero. Finally, it is generally assumed that entrainment of liquid in the gas flow is not feasible without a velocity difference between the phases:

$$\lim E_{\dot{x}\to 0} = 0 \quad \lim E_{\dot{x}\to 1} = 1 \quad \lim E_{p\to p_{crit}} = 0. \qquad [8]$$

An entrainment equation, which meets all the three limits and, additionally, accounts for the correct dependence on Reynolds and Weber number, reads as follows

$$E = \epsilon_E \cdot S_E \cdot S = 1 - \frac{(1-\dot{x})}{(1-\omega)(1-\dot{x})+\omega}; \quad \omega = f(\mathrm{Re}, \mathrm{We}). \qquad [9]$$

Here, ϵ_E is the mean volumetric entrainment and S_E, respectively, S are slip ratios. S_E accounts for the slip between the entrained liquid and the gas flow, and with S the relative velocity between

†This model is one of the few, which is not based on experimental data and, hence, it is not *a priori* constraint to a certain parameter range. A consideration of reasonable boundary limits for the slip ratio was the goal to a straightforward development of the equation (Schmidt 1993, p. 144).

‡In comparison to Ishii and Kataoka (1982) the exponent 1/3 used for the density correction term $(\rho_L - \rho_G)/\rho_G$ is neglected for the definition of the here used Weber number.

the liquid film and gas flow is taken into consideration disregarding the entrained liquid ($S = w_G/w_L$). Here, entrained liquid and gas are assumed to flow with equal (mean) velocities ($S_E = 1$). The unknown function ω has been fitted to pressure drops measured in horizontal and vertical upward air/water-flow to obtain $\omega = 0.18\ We^{0.12}Re^{0.50}$. Rearranging [9] leads to the mean volumetric liquid fraction entrained in the gas core, table 4, [19]. The dimensionless numbers We and Re in [20] of table 4 are defined with the inner pipe diameter d of the considered cross section, σ^* and η denote the surface tension and the dynamic viscosity of the liquid phase, respectively.

5.2. *Plane reaction force term*

A calculation of the plane reaction force requires the pressure acting on the annular plane of the pipe contraction as a function of all relevant flow parameters. Since it is impossible to determine this pressure analytically, the plane reaction force was empirically determined. However, it should keep to the following (theoretical) boundary limits: at a here assumed constant pressure within each flow area of the pipe, respectively, the core of the jet in the separated flow region the pressure immediately in front of the flow separation equals the inlet pressure p_1; further downstream it decreases to the pressure p_2 in the transitional cross section. The mean pressure on the annular area of the contraction should, therefore, lie inbetween these limiting values:

$$p_{base} = p_1 - \Gamma_{con}(p_1 - p_2); \quad \text{with } 0 \leqslant \Gamma_{con} \leqslant 1. \tag{10}$$

In this equation, Γ_{con} is the (dimensionless) base pressure coefficient. It has to be determined experimentally and is supposed to range inbetween the boundary limits 0 and 1. Equation [10] is less suitable for evaluating the base pressure from experimental values, since the pressure p_2 in the transitional cross section is not accurately measurable. Therefore, using the reliable measurable and in most cases only slightly lower outlet pressure p_3 is more favorable. In a (fictitious) frictionless flow without any flow separation both pressures would equalize. Herewith, the definition of the base pressure coefficient becomes:

$$\Gamma_{con} = \frac{p_1 - p_{base}}{p_1 - p_3} \quad \text{with } 0 \leqslant \Gamma_{con} < 1. \tag{11}$$

Following this equation a determination of the base pressure coefficient from experiments would, unfortunately, lead to an ambiguous result, because the distances of the cross sections 1 and 3 to the transitional cross section 2 are not unequivocally defined. Both cross sections are supposed to be close to the transition in a region of non-separated pipe flow. Therefore, the base pressure coefficient may be related directly to the (slightly smaller) pressure drop across the pipe contraction instead of selecting the pressure difference $p_1 - p_3$. In this case the coefficient is not constrained to values between zero and unity, but the overall dependency on flow parameters is the same

$$\Gamma_{con} \cong \frac{p_1 - p_{base}}{\Delta p_{con}}. \tag{12}$$

As experience shows, the base pressure coefficient depends mainly on the area ratio. On rearranging [4] the plane reaction force reads:

$$\Delta F_{base} = -\int_{A_3 - A_1} (p_1 - p_{base}(r))\mathrm{d}A = -[p_1 - p_{base}] \int_{A_3 - A_1} \mathrm{d}A = -\Gamma_{con}\Delta p_{con}[A_1 - A_3]. \tag{13}$$

The still unknown base pressure coefficient can be directly determined from experimental data taken with low viscosity fluid flow ($\Delta F_{fric} = 0$) in a horizonal direction ($\Delta F_{grav} = 0$) by using [3]

$$\Gamma_{con} = \frac{\sigma_{3,1}}{1 - \sigma_{3,1}} \left(\frac{\dot{m}_3^2 (1 - \sigma_{3,1} \dfrac{\rho_{eff,3}}{\rho_{eff,1}})}{\rho_{eff,3} \Delta p_{con}} - 1 \right). \tag{14}$$

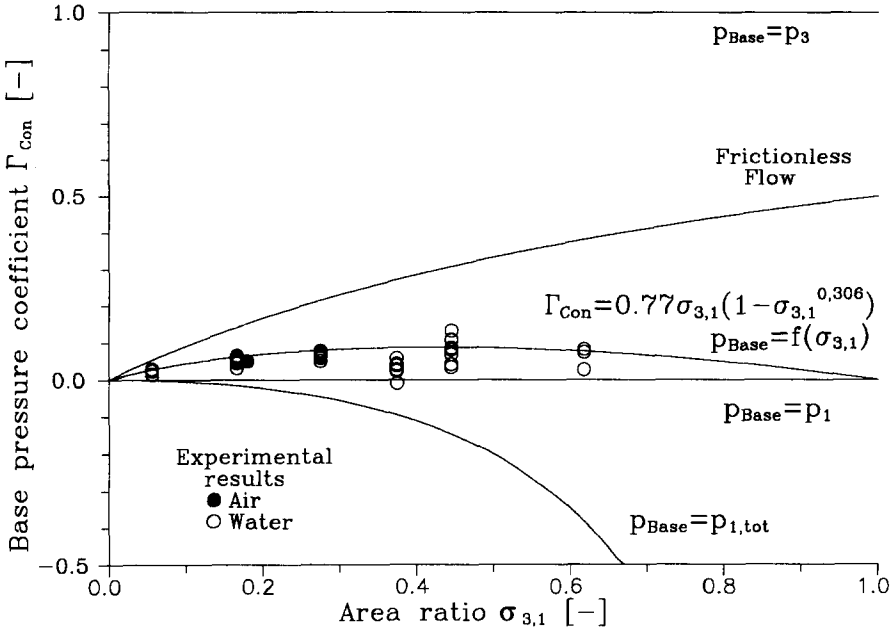

Figure 11. Base pressure coefficient as a function of the area ratio obtained from experimental results in air and in water flow and calculated by simplified assumptions about the mean base pressures.

$\sigma_{3,1}$ is defined as the area ratio A_3/A_1. In figure 11 the experimentally determined base pressure coefficient is given vs the area ratio of the pipe contraction. Additionally, theoretical boundaries for an incompressible fluid ($\rho_{\text{eff},1} = \rho_{\text{eff},3}$) are shown, e.g. the course of the base pressure coefficient in a frictionless flow through a contraction with $\Delta p_{\text{con}} = \dot{m}_3^2/2/\rho_{\text{eff},3}(1 - \sigma_{3,1}^2)$ and, subsequently, $\Gamma_{\text{con}} = \sigma_{3,1}/(1 + \sigma_{3,1})$. On the other hand, the assumption of the mean base pressure on the annular plane equal to the total (stagnation) pressure $p_{1,\text{tot}} = p_1 + \dot{m}_1^2/2/\rho_{\text{eff},1}$ in the inlet pipe would lead to the following equation for the base pressure coefficient†: $\Gamma_{\text{con}} = \sigma_{3,1}^2/(\sigma_{3,1}(1 + \sigma_{3,1}) - 2)$. In between these two limiting curves a new equation has been found as a best fit of the own experimental single-phase flow data, table 4, [21]. In the open literature a dependency of the base pressure coefficient on the area ratio is not considered, because it is generally assumed for simplicity that the mean base pressure p_{base} equals the mean pressure in the transitional cross section p_2 respectively the mean pressure in the outlet pipe p_3, if the pipe frictional pressure drop and the pressure change due to gravity are neglected. This leads to a value of unity for the base pressure coefficient independent of the area ratio.

The predicted results are in reasonable agreement with the mean base pressures determined from the measured pressure profile on the annular plane of a contraction with an area ratio of 0.1804 (Schmidt 1993) and with the results obtained by Teyssandier and Husain (1987) and Shouman and Massey (1968) at larger area ratios. The data of Teyssandier and Husain had been obtained in air flow through an orifice plate, whereas Shouman and Massey presented data of the pressure change at the annular face of sudden contractions with area ratios of 0.25 and 0.44. He also used air in his experiments.

5.3. *Friction force term*

For the prediction of the friction force term a (total) friction factor f_{con} is defined by introducing the velocity difference of the gas and liquid phase as the characteristic velocity

$$f_{\text{con}} = \frac{\Delta F_{\text{fric}}}{A_3 \frac{\rho_{\text{eff},3}}{2}[w_{G,3} - w_{L,3}]^2} = \frac{\Delta F_{\text{fric}}}{\frac{\dot{m}_3^2 \cdot \rho_{\text{eff},3}}{2}\left[\frac{\dot{x}}{\rho_{G1,3}\epsilon_3} - \frac{1-\dot{x}}{\rho_L(1-\epsilon_3)}\right]^2 A_3}. \quad [15]$$

†The friction and gravity forces in the inlet and outlet pipe are, for simplicity, neglected in the here considered momentum balance (see [3]).

Table 5. Definition of statistical numbers to evaluate the predictive accuracy of pressure drop models

Logarithmic ratio between measure and predicted pressure drop	Average of logarithmic ratios (n = Number of experimental values)	Standard deviation of logarithmic ratios (f = Number of variables)
$x_{\ln,i} = \ln\left(\frac{\Delta p_{i,\exp}}{\Delta p_{i,\mathrm{cal}}}\right)$	$\bar{x}_{\ln} = \exp\left\{\frac{1}{n}\sum_{i=1}^{n} x_{\ln,i}\right\} - 1$	$s_{\ln} = \exp\left\{\sqrt{\frac{\sum_{i=1}^{n} x_{\ln,i}^2}{(n-f-1)}}\right\} - 1$

In the case of gas or liquid flow the friction factor should be identical to that valid for the respective single-phase flow. If the velocities of both phases are equal ($w_G = w_L$), e.g. in homogeneous two-phase flow, the friction force term is zero, irrespective of the value of the friction factor.

The friction factor was fitted to measured pressure drop data from experiments with mixtures of air and aqueous glycerol respectively watery calcium nitrate, table 4, [22].

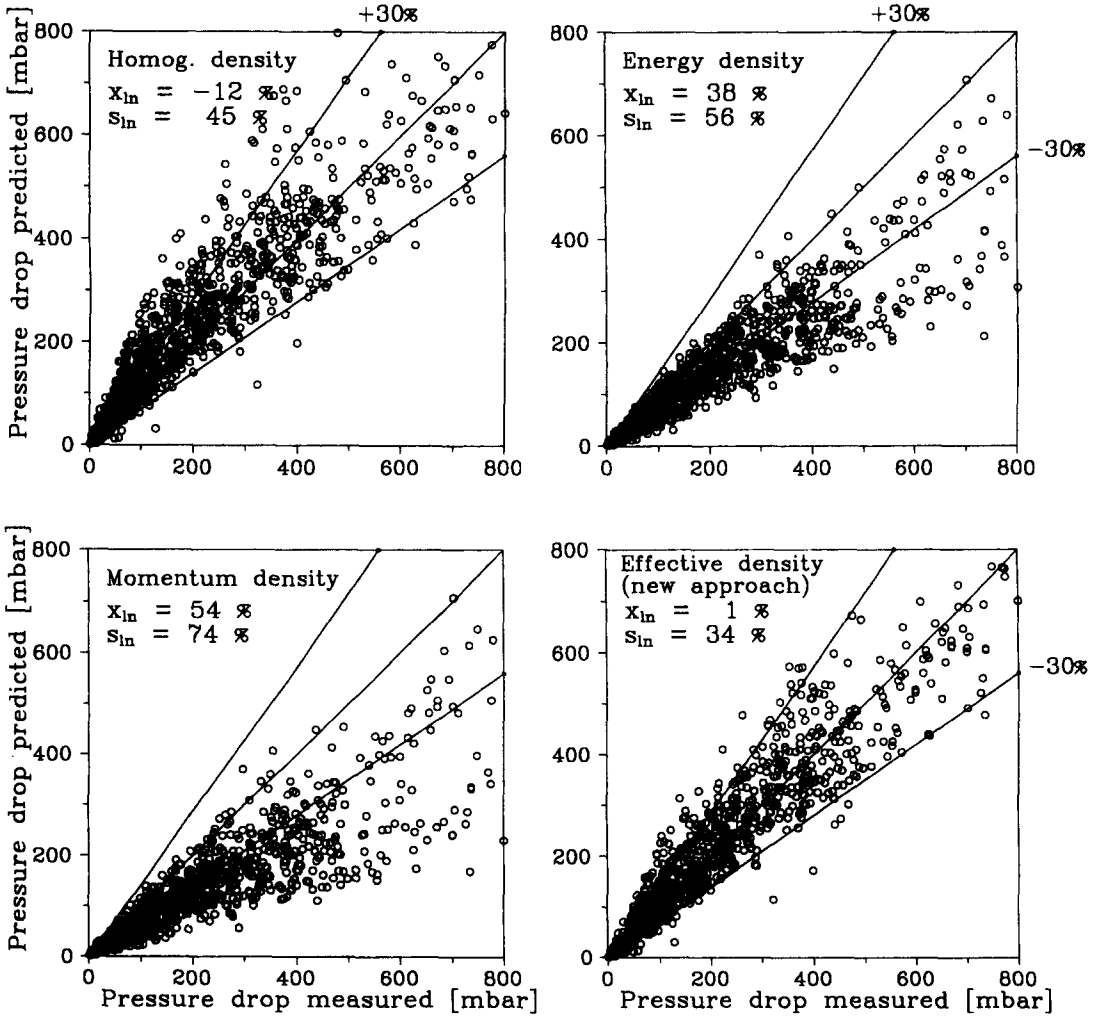

Figure 12. Reproductive accuracy of two-phase pressure drop models for pipe contractions.

Table 6. Basic pressure drop equation with alternative two-phase density definitions and a model to evaluate the contraction coefficient

$$\Delta p_{con} = \frac{\dot{m}_{VC}^2}{2\rho_{2ph}}[(1 - 1\sigma_{3,1}^2 C_C^2) - 2C_C(1 - C_C)].$$

Contraction coefficient according to Ruffell (1978):

$$C_C = 1 - \frac{1 - \sigma_{3,1}}{2.080\,(1 - \sigma_{3,1}) + 0.5371}$$

	Two phase density ρ_{2ph}
Momentum density	$\frac{1}{\rho_{mom}} = \frac{\dot{x}^2}{\rho_G \epsilon} + \frac{(1-\dot{x})^2}{\rho_L(1-\epsilon)}$
Homogeneous density	$\frac{1}{\rho_{hom}} = \frac{\dot{x}}{\rho_G} + \frac{1-\dot{x}}{\rho_L}$
Energy density	$\frac{1}{\rho_{energ}} = \left(\frac{\dot{x}}{\rho_G} + \frac{1-\dot{x}}{\rho_L}\right)^{-1}\left(\frac{\dot{x}^3}{\rho_G^2\epsilon^2} + \frac{(1-\dot{x})^3}{\rho_L^2(1-\epsilon)^2}\right)$

6. EVALUATION OF THE MODEL

The reproductive accuracy of the new model is compared to models in the open literature on the basis of two dimensionless statistical numbers: The average and the standard deviation x_{ln} and s_{ln} of the logarithmic ratios of measured (subscript exp) and predicted (subscript cal) pressure changes according to the definitions given in table 5. A discussion on the merits of these numbers in comparison to others used in statistics is given by Schmidt (1993).

The deviations obtained between measured and predicted pressure drops are shown in figure 12. Here, the own experimental results taken with mixtures of air and water respectively aqueous glycerol or calcium nitrate as well as freon 12 flow are considered (921 data points). Additionally, the data from the following authors are taken into consideration: 60 data points from Ferrel and McGee (1966) and McGee (1966), 53 from Fitzsimmons (1964), 60 from Geiger (1964), 75 from Heckle (1970a, 1970b) and 97 data points from Janssen (1966). All measurements were performed in steam/water-flow, except the experiments of Heckle (1970a, 1970b); he had used an air/water mixture. The experimental data of Husain (1975) have not been considered, because he recalculated them to correct for own measurement errors—the pressure tap located in the outlet pipe was not installed in the region of fully developed pipe flow. Data from Straub and Silberman (1960) have also been omitted, because they were not available in tabulated form. Considering the parity plot of figure 12, the average of the logarithmic ratios between measured and predicted values amounts to less than 1%, the standard deviation equals 34%. Indeed, measured pressure drops and calculational results from the new model are generally in quite good agreement. In comparison to the various models from the open literature the reproductive accuracy of the new model is by far better: beside the models depicted in table 6, the equations of Chisholm (1968), Ferrel and McGee (1966), Fitzsimmons (1964), Geiger (1964), Guglielmini *et al.* (1986), Husain (1975), Janssen (1966) and Richardson (1958) have been tested. Most of these authors have recommended a homogeneous flow model to calculate the pressure drop, although they agreed that this is physically not correct; the assumption of equal mean velocities of gas and liquid phase implied by the homogeneous flow model is highly questionable (see Ferrel and McGee 1966). Additionally, a flow contraction downstream of the transitional cross section in analogy to single-phase liquid flow is assumed and the liquid flow contraction coefficient is used for simplicity. Overall, the reproductive accuracy of these models are significantly lower than that of the new model.

Further improvements in the predictive accuracy seem to be realizable only, if an adequate prediction of the flow pattern in the inlet and outlet pipe is possible. Then, a more precise modeling of the void fraction, the volumetric liquid entrainment and the plane reaction force term as well as the friction force term depending on flow patterns might be feasible.

7. CONCLUSION

The pressure drop across a sudden contraction in a duct area has been measured with mixtures of air and water, aqueous calcium nitrate, watery glycerol and with the freon 12 in dependence of the most relevant physical parameters: flow direction (horizontal/vertical upward), mass flow quality, mass flux, area ratio and density and viscosity of the gas and the liquid phase. In total, about 1000 experiments were performed with eight test sections.

From measurements of the location and size of the narrowest cross section in pipe contractions it was concluded that unlike single-phase flow a two-phase flow does not contract behind the edge of the transition at least in a range of mass flow quality between 1 and 97%. Consequently, the contraction coefficient seems at least in two-phase flow not to be a physically reasonable parameter and should, therefore, not be used as intermediate parameter to calculate the two-phase pressure drop.

Based on momentum and mass balances as well as on experimental results a new pressure drop model has been developed. Herein, for the first time the amount of entrained liquid is taken into consideration. In comparison to the models in the open literature the new equation includes more relevant parameters: the compressibility of the two-phase flow, the change of mean void fraction, the viscosity of the gas and liquid phase and the surface tension. Additionally, the model meets all of the relevant theoretical boundary values.

The model predicts the experimental results sufficiently accurate for engineering purposes, 80% of all available data (own data and results available in the literature) were predicted within $\pm 30\%$. The parameter ranges cover a wide range of conditions, pipe diameters and physical properties typically encountered in industrial piping systems. Beyond the investigated parameter range a moderate extrapolation should be permissible, since boundary limits have been taken into consideration.

REFERENCES

Chisholm, D. (1968) Prediction of pressure losses of changes of section, bends and throttling devices. NEL Rep. 388.

Ferrell, J. K. and McGee, J. W. (1966) Two-phase flow through abrupt expansions and contractions. North Carolina State Univ. USAEC, Contract No. AT-(40-1)-2950, pp. 1–163.

Fitzsimmons, D. E. (1964) Two-phase pressure drop in piping components. Engng Develop. Operation, Handford Lab., HW-80970 REV1, pp. 1–59.

Geiger, G. E. (1964) Sudden contraction losses in single and two-phase flow. Ph.D. thesis, Univ. Pittsburgh, 65–79.

Guglielmini, G., Lorenzi, A., Muzzio, A. and Sotgia, G. (1986) Two phase flow pressure drops across sudden area contractions. *Proc. 8th Int. Heat Transfer Conf.*, Vol. 5, pp. 2361–2366.

Heckle, M. (1970) Bestimmung der Zweiphasenströmung Gas/Flüssigkeit durch Drosselorgane. *Chem.-Ing.-Techn.* **42**, 304–310.

Heckle, M. (1970) Zweiphasenströmung Gas/Flüssigkeit durch Drosselorgane. *Fortschr.-Ber. VDI Zeitschr.* **3**, 1–97.

Huq, R. (1990) An analytical two-phase flow void prediction method. *AIAA/ASME 5th Joint Thermophysics and Heat Transfer Conf.*, Paper No. 90-1738.

Husain, A (1975) Applicability of the homogeneous flow model to two-phase flow. Ph.D. thesis, Univ. Cincinnati.

Ishii, M. and Kataoka, I. (1982) Hydrodynamics of annular flow. *Proc. ASME PVP Conf.*, Orlando, Florida.

Janssen, E. (1966) Two phase pressure loss across abrupt contractions and expansions, steam water at 600 to 1400 psia. *Int. Heat Transfer Conf.*, pp. 12–23.

Kays, W. M. (1950) Loss coefficients for abrupt drops in flow cross section with low Reynolds number flow in single and multiple-tube systems. *Trans. ASME* **73**, 1068–1074.

McGee, J. W. (1966) Two-phase flow through abrupt expansions and contractions. Ph.D. thesis, North Carolina State Univ. at Raleigh.

Morris, S. D. (1990) Discharge coefficients for choked gas-liquid flow through nozzles and orifices and applications to safety devices. *J. Loss Prev. Process Ind.* **3**, 303–310.

Morris, S. D. (1984) A simple model for estimating two-phase momentum flux. *1st U.K. Nat. Conf. on Heat Transfer* **2**, 773–784.

Richardson, B. L. (1958) Some problems in horizontal two-phase two-component flow. Ph.D. thesis, Univ. Chicago.

Rouhani, S. Z. (1974) Modified correlations for void fraction and two phase pressure drop. AE-RTV-841, 1974.

Rousseau, J. C. (1986) Flashing flow. *Multiphase Sci. Technol.* **3**, 378–389.

Ruffell, A. E. (1978) Calculation of pressure loss coefficients for pipework contractions. NEDR/10/0035, Issue No. 1, 1–2.

Schmidt, J. (1993) Berechnung und Messung der Druckänderungen über plötzliche scharfkantige Rohrerweiterungen und -verengungen bei Gas/Dampf-Flüssigkeitsströmung. Fortschr.-Ber. VDI. Reihe 7 Nr. 236. VDI-Verlag, Düsseldorf, Germany.

Shouman, A. R. and Massey, J. L. Jr (1968) Stagnation pressure losses of compressible fluids through abrupt area drops neglecting friction at the walls. ASME Pap. 68-WA/FE-46.

Straub, L. and Silberman, E. (1960) Air–water mixture flow through orifices, bends, and other fittings in a horizontal pipe. St. Anthony Falls Hydraulic Lab., Report No. 63.

Teyssandier, R. G. and Husain, Z. D. (1987) Experimental investigation of an orifice meter pressure gradient. *J. Fluids Engng, Trans. ASME* **109**, 144–148.

Whalley, P. B. and Ward, J. A. (1981) The calculation of void fraction in two-phase flow. HTFS Design Report, Part 4, AERE-R 9792.